Chinese Journal of
POLYMER SCIENCE

RESEARCH ARTICLE

https://doi.org/10.1007/s10118-026-3761-z
Chinese J. Polym. Sci.

Bioinspired Zinc-doped Nano Hydroxyapatite Reinforced Poly(lactic acid) Composites for Bone Repair

Hong-Xiang Yin[a,†], Yang Wang[a,b,†], Yi-Fei Wu[a], Jin-Jing Li[a], Xiao Kong[a], Wen-Hao Mei[a], Ze-Tong Wang[a], Chun-Sheng Xiao[b], Cheng Zhang[c*], Zhan-Fu Cong[d], Irshad Hussain[e], Zhao-Hui Tang[b*], and Wei Yan[a*]

[a] *Key Laboratory of Green Preparation and Application for Functional Materials of Ministry of Education, Hubei Key Laboratory of Polymer Materials, School of Material Science and Engineering, Hubei University, Wuhan 430062, China*
[b] *State Key Laboratory of Polymer Science and Technology, Key Laboratory of Polymer Ecomaterials, Changchun Institute of Applied Chemistry, Chinese Academy of Sciences, Changchun 130022, China*
[c] *School of Life Science, Hubei University, Wuhan 430062, China*
[d] *Changchun SinoBiomaterials Co., Ltd., Changchun 130103, China*
[e] *Department of Chemistry and Chemical Engineering, SBA School of Science and Engineering, Lahore University of Management Sciences (LUMS), DHA, Lahore 54792, Pakistan*

Electronic Supplementary Information

Abstract Bone defects remain a major clinical challenge due to the slow rate of recovery, complex surgical procedures, and great impact on the lives of patients. Therefore, the development of biocompatible, durable, degradable artificial bone grafts is highly desirable. Inspired by the natural composition of human bone, this study reports the fabrication of poly(lactic acid) (PLA)/zinc-doped hydroxyapatite (Zn-HA) composite materials *via* the melt blending method. The chemical properties, mechanical performance, degradability, and biocompatibility of the composites were evaluated systematically. Among them, the 10 wt% PLA/Zn-HA composite exhibited optimal performance, including high tensile and flexural strengths, superior thermal stability, and the lowest degradation rate. Controlled degradation and sustained release of zinc ions further enhance osteoblast activity with low cytotoxicity. Furthermore, Alkaline Phosphatase (ALP) activity and Alizarin Red S (ARS) staining confirmed that the 10 wt% PLA/Zn-HA composite significantly promoted osteogenic differentiation. By simultaneously achieving mechanical reliability and enhanced biological properties, this study provides promising design criteria for next-generation artificial bone grafts for bone defect repair.

Keywords Bone repair; Poly(lactic acid); Zinc-doped hydroxyapatite; Composite materials

Citation: Yin, H. X.; Wang, Y.; Wu, Y. F.; Li, J. J.; Kong, X.; Mei, W. H.; Wang, Z. T.; Xiao, C. S.; Zhang, C.; Cong, Z. F.; Hussain, I.; Tang, Z. H.; Yan, W. Bioinspired zinc-doped nano hydroxyapatite reinforced poly(lactic acid) composites for bone repair. *Chinese J. Polym. Sci.* https://doi.org/10.1007/s10118-026-3761-z

INTRODUCTION

Bone defects have become a major health concern due to their slow rate of recovery, complex surgical procedures, and great impact on the lives of patients.[1–4] Bone grafts have predominantly been used for the treatment of bone defects.[5,6] Over two million bone grafting surgeries are conducted annually worldwide, making it the second most frequent tissue transplantation.[7,8] Traditionally bone grafts are classified into autologous bone grafts, allogeneic bone grafts, and artificial bone grafts.[9]

Autologous bone grafts have always been considered the "golden standard" for bone repair, but drawbacks such as limited supply and possible donor site complications limited their application.[10–12] As an effective alternative to autologous bone grafts, allogeneic bone grafts are widely used in the treatment of bone defects, which can avoid damage to the donor site bone structure. However, they still have disadvantages, such as insufficient supply, ethical controversies, and immune rejection. Utilizing natural or synthetic materials to simulate human bone properties, artificial bone grafts have been optimized to reduce immune rejection and infection risk. Although they can be easily acquired at low cost, current artificial bone graft materials still have poor biocompatibility and degradability, which may result from the introduction of metallic materials or unsatisfactory mechanical performance owing to the use of polymers.[13–16] Therefore more efforts should be made to develop biocompatible, degradable artificial bone graft materials with appropriate strength to meet the requirements of bone defect repair and benefit patients.[17]

To overcome the limitations of single-component materi-

* Corresponding authors, E-mail: zhangcheng1988@hubu.edu.cn (C.Z.)
E-mail: ztang@ciac.ac.cn (Z.H.T.)
E-mail: willieyan2003@hubu.edu.cn (W.Y.)
† These authors contributed equally to this work.
Received April 1, 2026; Accepted May 29, 2026; Published online July 20, 2026

als, composite materials have been developed to improve the mechanical, physicochemical, and biological properties of bone grafts.[18–21] Composite materials primarily include a combination of bioceramics and polymers. Diverse techniques and strategies have also been utilized to modify composite materials.[22–25] For instance, polymers, such as collagen and poly(lactic acid) (PLA), are widely used in bone tissue engineering because of their excellent biocompatibility and bone remodeling performance.[26–29] However, they exhibit poor mechanical properties and osteoinductivity.[30–34] Therefore, other components, such as ceramics, are often introduced to improve the porosity, stability, and osteogenic activity of composite matrices in bone regeneration.[35–38]

Human bones have both collagen fibers and a hydroxyapatite skeleton to simultaneously maintain strength and tenacity. Zinc (Zn) is an essential trace element in the human body. The incorporation of Zn into HA could help mimic the mechanical stability of bone and further promote cell growth and tissue regeneration through its biological effects. Based on the original bone formation, we selected PLA and Zinc-doped hydroxyapatite (Zn-HA). By combining polymers with ceramic compounds, excellent biocompatibility and mechanical and controllable degradation rates have been achieved. Additionally, the degradation of Zn can establish a mild microenvironment for osteogenesis and osteoinductivity in bone defects. This study provides a bioinspired PLA/Zn-HA-based strategy for bone tissue engineering and is expected to be used for bone defect regeneration.

EXPERIMENTAL

General Considerations

PLA was purchased from Changchun SinoBiomaterials Co., Ltd., and zinc-doped hydroxyapatite was purchased from Hubei Central Medical Technology Co., Ltd.

Preparation of PLA/Zn-HA

PLA/Zn-HA composites were prepared by melt blending at 110 r/min and 180 °C for 7 min (Scheme 1).

Characterization

A NcoletiS50 Fourier transform infrared spectrometer was used to analyze the functional groups in the materials. The sample was heated from room temperature to 800 °C at a heating rate of 10 °C/min under a nitrogen atmosphere.

A Q2000-type DSC analyzer was used to investigate the melting and crystallization behaviors. The samples were heated from 0 °C to 200 °C at a rate of 10 °C/min, held at 200 °C for 2 min, and finally cooled to 0 °C at a rate of 10 °C/min.

X-ray diffraction analysis was performed to study the crystal properties using a German Bruker D8 Advance X-ray diffractometer at a scanning speed of 4 (°)/min and scanning range of 10°–60°.

A universal tensile analyzer was used to measure the tensile, bending, and impact strengths and moduli of the composite materials at test rates of 50 mm/min, 2 mm/min and 2.9 m/s, respectively.

The morphology of the fracture surfaces of the tensile specimens was observed using a SIGMA 500 field-emission scanning electron microscope at an accelerating voltage of 10 kV.

RESULTS AND DISCUSSION

Characterization

The infrared spectra of the Zn-HA and PLA/Zn-HA composites with different formulation ratios were first evaluated (Fig. 1a). In

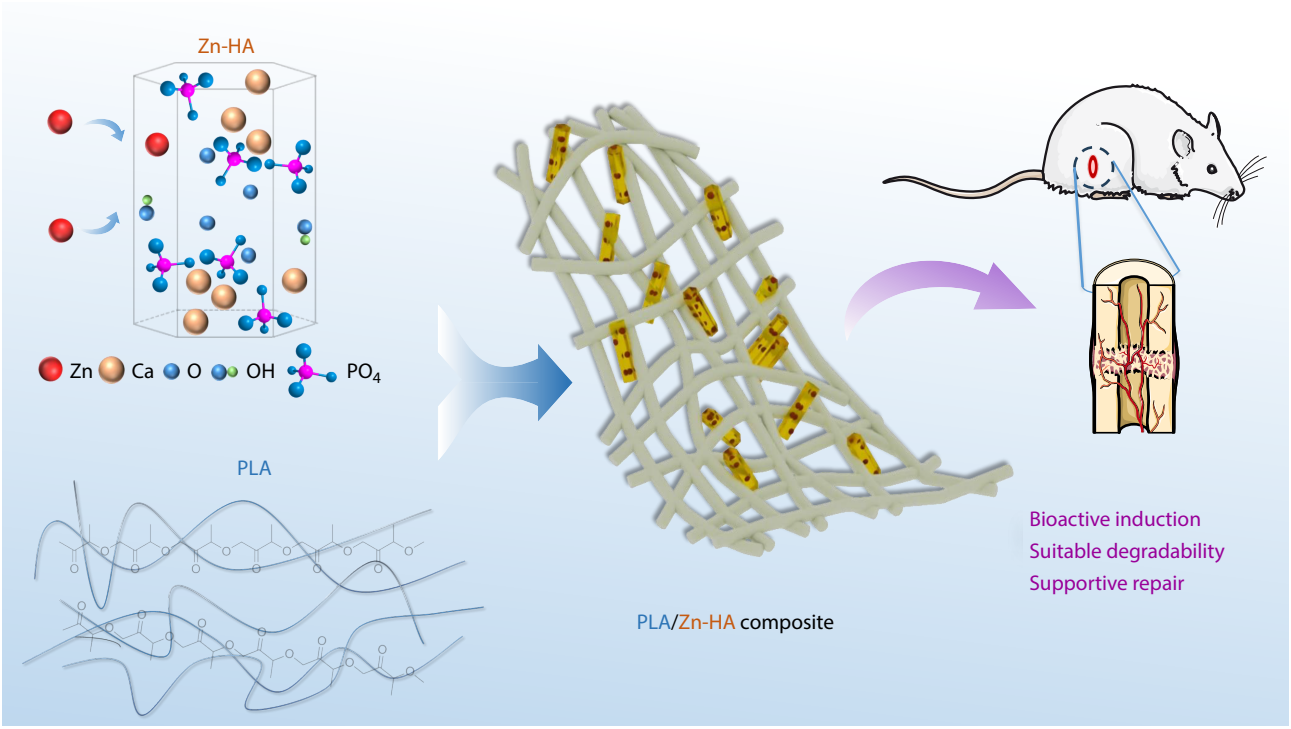

Scheme 1 Preparation of PLA/Zn-HA composite for bone repair.

https://doi.org/10.1007/s10118-026-3761-z

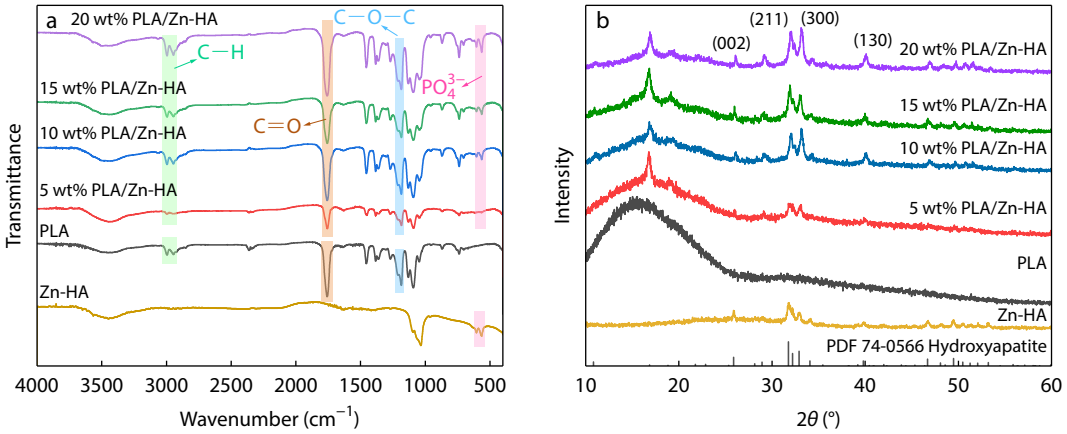

Fig. 1 Characterizations of PLA, Zn-HA and PLA/Zn-HA composites with different formulation ratios: (a) FTIR spectra, (b) XRD patterns.

the composite materials, the characteristic stretching vibrations of C=O, C—O—C, C—H in PLA can be observed (1759,1185 and 2944 cm^{-1}, respectively), as well as the $\gamma 4$ vibration characteristic peaks of phosphate groups in Zn-HA (563 and 605 cm^{-1}). Furthermore, as the Zn-HA content increased, The intensity of the $\gamma 4$ vibrations of the phosphate groups increased, confirming their coexistence.

XRD analysis was conducted to further elucidate the effects of Zn-HA on the crystallization of PLA (Fig. 1b). PLA, a semi-crystalline polymer, typically displays a broad peak around 2θ=16.8°. The addition of Zn-HA enhanced the sharpness of this peak, indicating a transition toward a highly crystalline state. As the Zn-HA content increased, the intensity of the characteristic peak at 2θ=16.8° also increased, demonstrating that Zn-HA particles serve as heterogeneous nucleating agents, increasing the overall crystalline fraction of the PLA matrix. However, excessive Zn-HA content may lead to particle agglomeration, reducing crystallization efficiency.

The diffraction peaks of the Zn-HA nanoparticles aligned with the hydroxyapatite standard (JCPDS 74-0566), confirming their crystalline structure. The incorporation of Zn-HA resulted in distinct peaks in the XRD patterns of the composites.

TGA was performed to evaluate the effect of Zn-HA on the thermal stability of PLA (Figs. 2a and 2b). All the samples were thermally stable at temperatures below 300 °C. The temperature corresponding to 5 wt% ($T_{5\%}$) mass loss in the undoped PLA was 303.8 °C. As the Zn-HA content increased, the $T_{5\%}$ of the composites initially increased, followed by a subsequent decrease; the respective values were 321.6, 331.8, 329.8, and 311.3 °C, (Table S2 in the electronic supplementary information, ESI). The composite with 10 wt% Zn-HA exhibited the highest $T_{5\%}$, indicating optimal thermal stability. The improved thermal stability at moderate Zn-HA concentrations can be attributed to the nucleating effect of Zn-HA, which promotes PLA crystallization. These results suggest that appropriate Zn-HA concentrations enhance the crystallization of the PLA matrix; however, excessive doping leads to particle agglomeration, which degrades interfacial compatibility.

When the temperature reached 600 °C, PLA completely decomposed, and the residue weight represented the actual concentration of Zn-HA, with residual weights of 4.4%, 10.8%, 14.2%, and 17.5%, closely matching the theoretical proportions, confirming the effective integration during melt blending.

DSC was used to assess the influence of Zn-HA on the crystallization behavior of the PLA/Zn-HA composites (Fig. 2c). The glass transition temperature (T_g) of the undoped PLA and the composites ranged from 57 °C to 59 °C, indicating the absence of a chemical reaction between PLA and Zn-HA. Zn-HA acted as a physical filler without altering the mobility of the PLA molecular chains. The cold crystallization transition temperature (T_{cc}) and melting temperature (T_m) of undoped PLA were 107.6 and 161.9 °C, respectively. The incorporation of Zn-HA decreased T_{cc} while increasing T_m, which can be attributed to the nucleation effects of Zn-HA.

The cooling curves of the PLA/Zn-HA composites exhibit a distinct crystallization peak compared to that of undoped PLA (Fig. 2d), further confirming that Zn-HA acts as an efficient nucleating agent. According to the DSC results, the crystallinity of the undoped PLA was calculated to be 31.4%. The highest crystallinity (39.5%) occurred at 10 wt% Zn-HA, indicating that optimal doping enhances the physicochemical properties of the composite by providing abundant nucleation sites that facilitate the crystalline order throughout the matrix, consistent with formulation ratios and thermogravimetric analysis.

SEM images of the fracture surface of undoped PLA appeared relatively smooth and flat (Fig. 3a). At a low Zn-HA loading of 5 wt% (Fig. 3b), the Zn-HA particles were homogeneously dispersed and remained well embedded after fracture. This uniform dispersion enhances the toughening effect of the inorganic rigid particles. At a Zn-HA concentration of 10 wt% (Fig. 3c), a uniform dispersion of Zn-HA was achieved. When the Zn-HA content continued to increase (Figs. 3d and 3e), pronounced particle agglomeration and non-uniform filler distribution became evident. These agglomerates act as stress concentration sites, potentially inducing stress concentration and subsequent crack propagation.

Tensile, bending, and impact tests were conducted to comprehensively evaluate the mechanical properties of the PLA/Zn-HA composites (Fig. 4). All experiments were performed in triplicates to ensure reproducibility. The tensile strength, flexural strength, and impact strength of undoped PLA were 61.5 MPa, 63.3 MPa, and 3.8 kJ/m^2, respectively. The addition of Zn-HA resulted in the initial enhancement of these properties, followed by a subsequent decline. For 10

https://doi.org/10.1007/s10118-026-3761-z

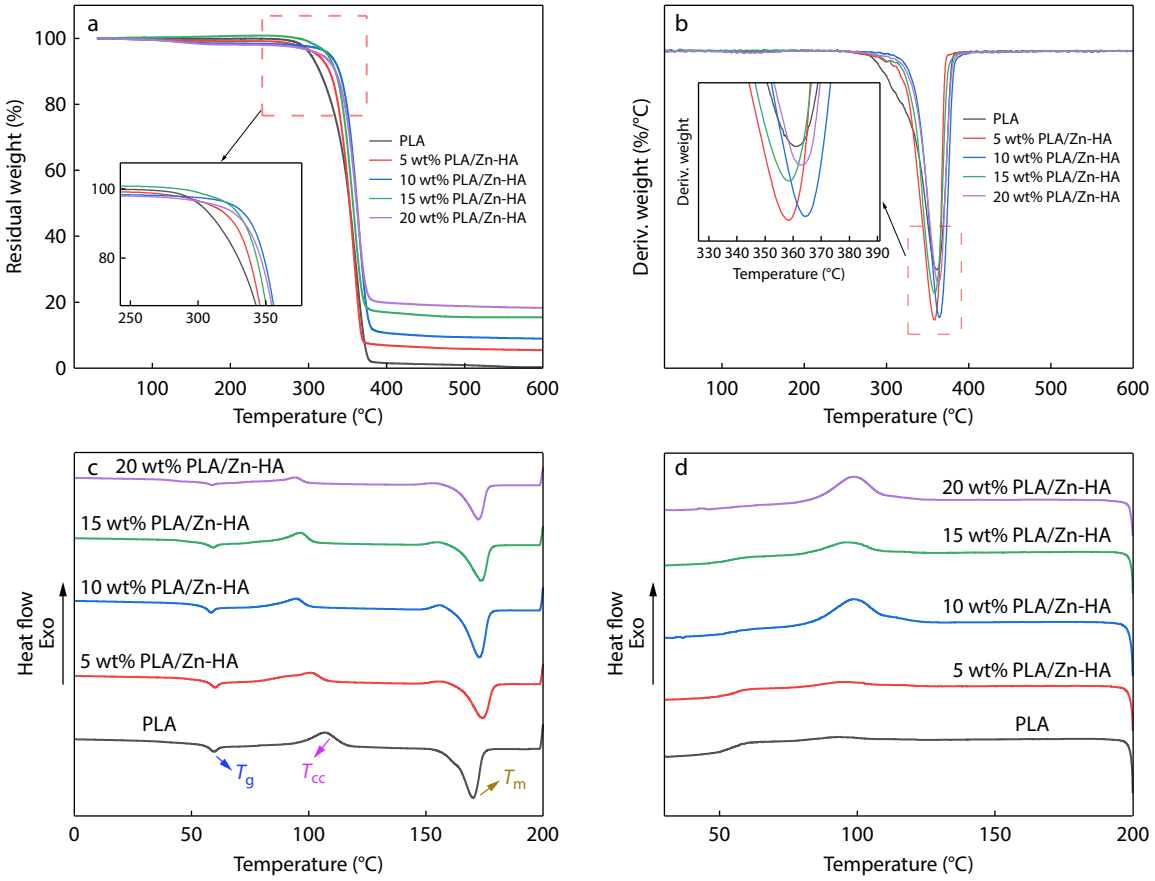

Fig. 2 Thermal analysis of PLA, Zn-HA and PLA/Zn-HA composites with different formulation ratios: (a) TG curves, (b) DTG curves, (c) DSC heating curves, (d) DSC cooling curves.

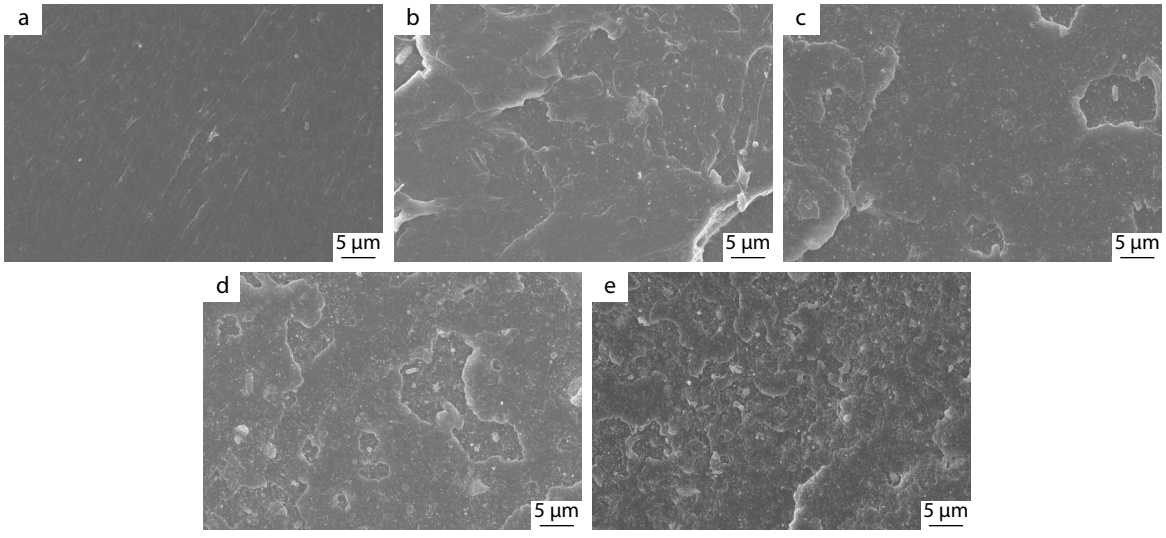

Fig. 3 Tensile fracture surface morphology of PLA/Zn-HA with different zinc-doped hydroxyapatite contents: (a) 0 wt%, (b) 5 wt%, (c) 10 wt%, (d) 15 wt%, (e) 20 wt%.

wt% Zn-HA, the composites achieved the highest tensile strength (63.2 MPa), flexural strength (64.7 MPa), and impact strength (4.3 kJ/m^2). At lower Zn-HA concentrations, owing to the interfacial incompatibility between PLA and Zn-HA, Zn-HA primarily functions as a microscopic defect and stress concentrator, leading to an initial decrease in tensile and flexural strength. Upon reaching an optimal loading of 10 wt%, a uniform dispersion of Zn-HA was achieved, which facilitated efficient stress transfer and dissipation throughout the polymer matrix. Above this optimum concentration (>10 wt%), the mechanical performance undergoes a subsequent decline. This decline can be attributed to the severe agglomeration of

Zn-HA, as corroborated by SEM observations. These substantial agglomerates not only weaken the structural integrity of the PLA matrix but also serve as intense stress concentration sites. Under the effect of external forces, cracks occur at these agglomerate interfaces and propagate rapidly, ultimately leading to a steady deterioration in the mechanical performance.

In bone grafting, materials degrade *in vivo*, and new bone tissue grows and gradually replaces the degraded portions. Ideally, the degradation rate of the scaffold should match the growth of the bone tissue. Therefore, *in vitro* degradation experiments are necessary to assess the suitability of PLA/Zn-HA composites for bone-repair applications. The flexural properties of the PLA/Zn-HA composites at different formulation ratios after 0, 5, 10, and 20 days of degradation were assessed (Fig. 5a). After 20 days, the tensile strength of undoped PLA decreased by 6.9%, from 62.1 MPa to 57.8 MPa. The flexural strength reductions for composites with 5 wt%, 10 wt%, 15 wt%, and 20 wt% Zn-HA were 7.5%, 5.5%, 7.1%, and 9.5%, respectively, demonstrating a trend of initial reduction followed by recovery. The composite with 10 wt% Zn-HA exhibited the best mechanical performance retention after degradation. Variations in the reduction rates among different Zn-HA contents indicate that the degradation rate of PLA can be modified by adjusting the Zn-HA content, allowing for tailored performance to meet specific requirements of the implantation site.

The Zn ion release amounts from the 10 wt% PLA/Zn-HA composite over 0, 5, 10, and 20 days of degradation were assessed (Fig. 5b). The Zn ion release initially increased with degradation time before and exhibited a subsequent plateau or downward trend. This decline is attributed to the depletion of surface-accessible Zn ions. Once the surface Zn was exhausted, the release of ions from the internal matrix was restricted by the surrounding PLA matrix, resulting in a reduction in the overall release rate.

Biocompatibility and Bioactivity

Osteoblasts, the primary functional cells of bone tissue, play a crucial role in bone formation and repair. Therefore, we selected the mouse osteoblast cell line (MC3T3) to evaluate its cytocompatibility. The viability of MC3T3 cells in the extract of the 10 wt% PLA/Zn-HA composite ranged from 99.5% to 91.0% at extract concentrations of 0.1 mg/mL to 0.8 mg/mL (Fig. 5c), demonstrating excellent cytocompatibility.

Alkaline Phosphatase (ALP) and Alizarin Red S (ARS) staining assays were performed to comprehensively evaluate the osteogenic capacity and bone regeneration potential of the composite material (Figs. 6a–6d). Alkaline Phosphatase, an early marker of osteogenic differentiation during cellular mineralization, was used to evaluate the osteogenic potential of the materials using ALP staining and activity assays. ALP analysis on days 7 and 14 revealed that the composite material containing 10 wt% PLA/Zn-HA exhibited the highest enzyme activity at both time points (Fig. 6c), which was significantly higher than that of the pure PLA, 10 wt% PLA/HA, and other

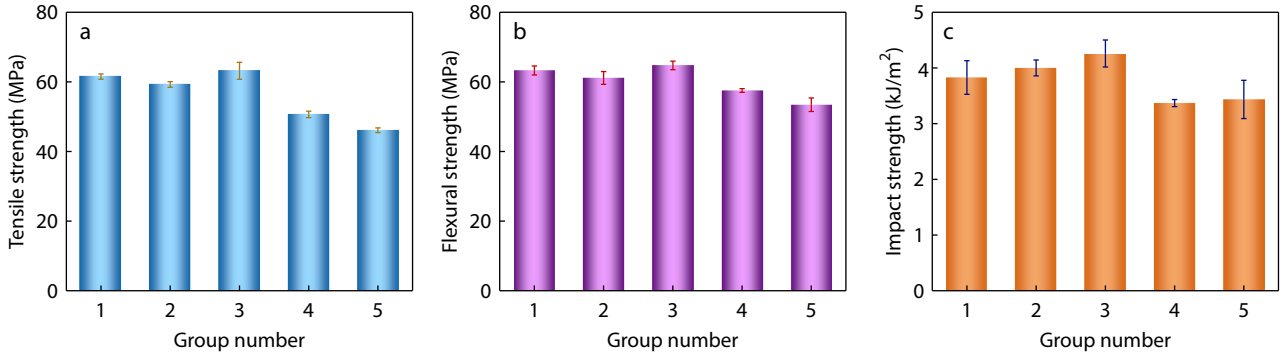

Fig. 4 Mechanical properties of PLA/Zn-HA composites with different formulation ratios: (a) tensile strength, (b) flexural strength, (c) impact strength (1, 2, 3, 4, and 5 represent 0 wt% Zn-HA, 5 wt% Zn-HA, 10 wt% Zn-HA, 15 wt% Zn-HA, 20 wt% Zn-HA, respectively).

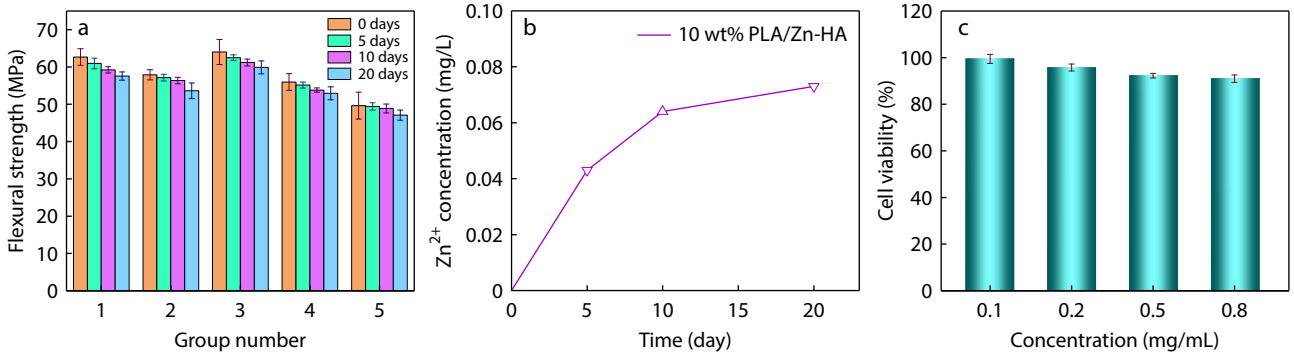

Fig. 5 *In vitro* degradation tests and cell viability on MC3T3 cells of 10 wt% PLA/Zn-HA. (a) The flexural strength attenuation of PLA/Zn-HA composite materials with different formulation ratios after degradation; (b) The zinc ion release amount of the 10 wt% PLA/Zn-HA composite material after degradation; (c) Cell viability of 10 wt% PLA/Zn-HA.

https://doi.org/10.1007/s10118-026-3761-z

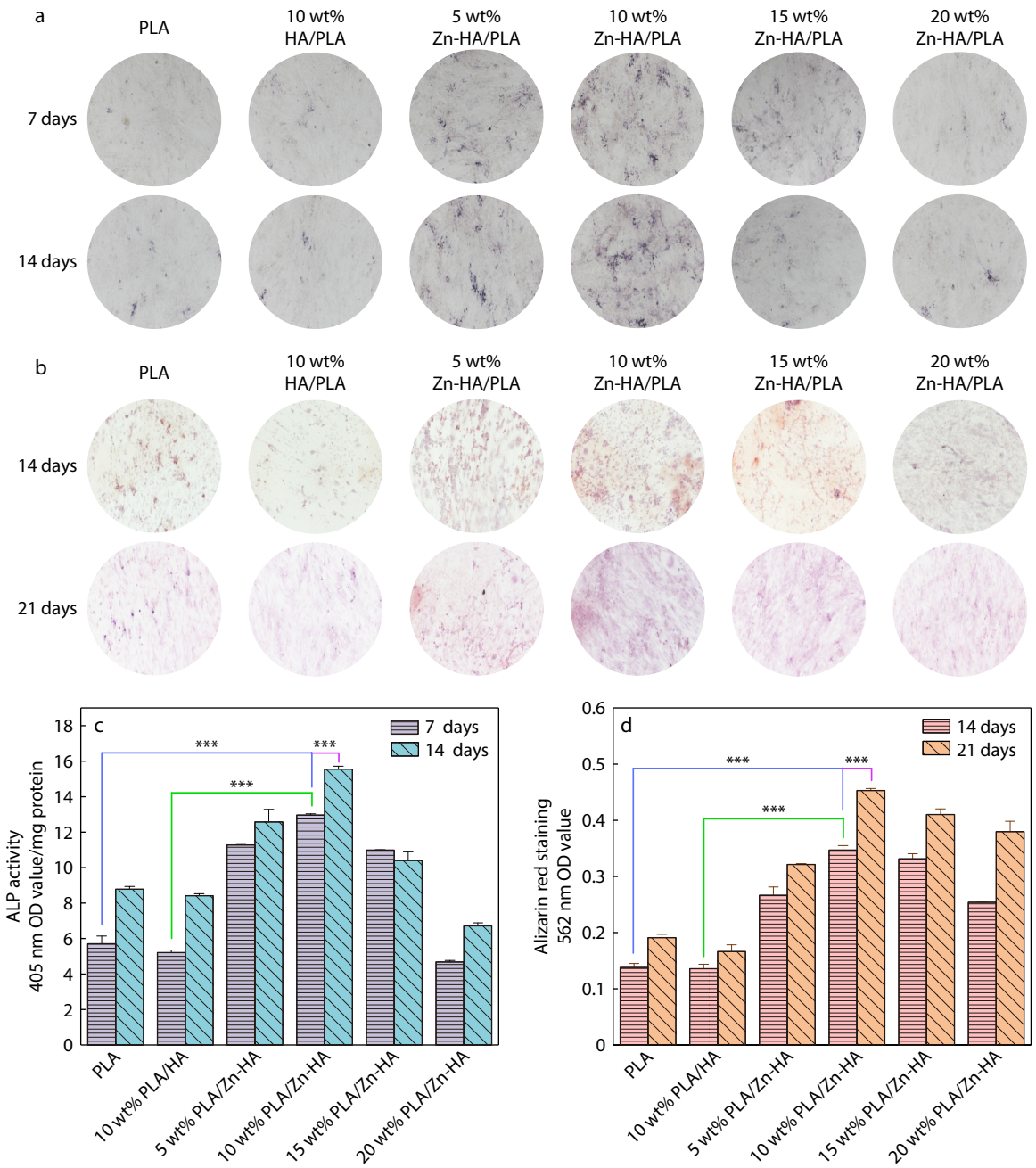

Fig. 6 Osteogenic differentiation of MC3T3 cells cultured on PLA and composite films. (a) Representative alkaline phosphatase (ALP) staining images on day 7 and day 14; (b) Representative Alizarin Red S (ARS) staining images of mineralized nodules on day 14 and day 21; (c) ALP activity on day 7 and day 14; (d) OD values of ARS staining on day 14 and day 21. All quantitative data are presented as mean ± SD (n=3). *** p< 0.001.

control groups (***p<0.001). Notably, at the same 10 wt% doping concentration, the Zn-doped composite material markedly enhanced ALP expression compared to the HA control without Zn, further confirming that Zn incorporation effectively promotes osteogenic differentiation.

Alizarin Red S staining was used to assess calcium deposition. These results demonstrated markedly enhanced calcium deposition in the Zn-HA groups (Fig. 6d). The 10 wt% Zn-HA formulation produced the highest absorbance values on days 14 and 21 (***p<0.001). The corresponding microscopic images of the stained cultures further supported the quantitative findings. The 10 wt% PLA/Zn-HA group exhibited denser cell clusters and more intense red staining than PLA and 10 wt% PLA/HA, indicating accelerated nodule formation and matrix mineralization. These results demonstrated that the 10 wt% PLA/Zn-HA composite provided optimal osteogenic induction, positioning it as a promising candidate for bone repair applications.

CONCLUSIONS

In summary, a series of PLA/Zn-HA composite materials with dif-

ferent amounts of Zn-HA were precisely fabricated and tailored, and their physicochemical and mechanical properties, degradability, and biocompatibility were comprehensively evaluated. *In vitro* degradation experiments demonstrated that the mechanical properties and degradation rate of the PLA/Zn-HA composite material could be modulated by varying the content of Zn-HA to accommodate the specific requirements of various implantation sites. The 10 wt% PLA/Zn-HA composite material emerged as the optimal composite, exhibiting the best thermal stability, the highest mechanical properties (tensile strength of 63.2 MPa, flexural strength of 64.7 MPa, and impact strength of 4.3 kJ/m^2), the lowest decrease in flexural performance after degradation (5.5%). Biocompatibility evaluations confirmed that the 10 wt% PLA/Zn-HA composite exhibited better cell proliferation, differentiation, and osteogenic ability. The PLA/Zn-HA composite could achieve favorable mechanical performance, bioactivity, and adjustable degradability, providing a potent platform for the repair of critical bone defects.

Conflict of Interests

The authors declare no interest conflict.

Electronic Supplementary Information

Electronic supplementary information (ESI) is available free of charge in the online version of this article at http://doi.org/10.1007/s10118-026-3761-z.

Data Availability Statement

The related data of this study can be obtained from the authors for reasonable reasons. Author's contact information: willieyan2003@hubu.edu.cn.

ACKNOWLEDGMENTS

This study was financially supported by the National Key R&D Program of China (No. 2022YFC 2405800).

REFERENCES

1 Shen, N.; Zhang, Z.; Wu, F.; Zhu, Z.; Liu, J.; Qi, X.; Li, Q.; Wang, X.; Ma, Q.; Xiang, H. Advances in self-powered biomaterials for bone defect repair. *Adv. Compos. Hybrid Mater.* **2024**, *8*, 38.
2 Chen, N.; Luo, F.; Yang, G.; Yao, J.; Chen, X.; Shao, Z. Production of functional materials derived from regenerated silk fibroin by utilizing 3d printing and biomimetic enzyme-induced mineralization. *Chinese J. Polym. Sci.* **2024**, *42*, 299–310.
3 Yu, Y.; Chen, R.; Chen, X.; Wang, J.; Liu, C. Regulating the bioactivity of non-glycosylated recombinant human bone morphogenetic protein-2 to enhance bone regeneration. *Bioact. Mater.* **2024**, *38*, 169–180.
4 Chen, R.; Wang, J.; Liu, C. Biomaterials act as enhancers of growth factors in bone regeneration. *Adv. Funct. Mater.* **2016**, *26*, 8810–8823.
5 Xue, P.; Wang, J.; Fu, Y.; He, H.; Gan, Q.; Liu, C. Material-mediated immunotherapy to regulate bone aging and promote bone repair. *Small* **2025**, *21*, 2409886.
6 Wei, W.; Dai, H. Articular cartilage and osteochondral tissue engineering techniques: recent advances and challenges. *Bioact. Mater.* **2021**, *6*, 4830–4855.
7 Chen X, C. H. in *Biomedical polymers*. China Science Press, Beijing, **2018**, p. 22–29.
8 Chen X. in *Degradable medical polymer materials*. China Science Press, Beijing, **2020**, p. 43–47.
9 Derksen, W.; Joda, T.; Chantler, J.; Fehmer, V.; Gallucci, G. O.; Gierthmuehlen, P. C.; Ioannidis, A.; Karasan, D.; Lanis, A.; Pala, K.; Pjetursson, B. E.; Roccuzzo, M.; Sailer, I.; Strauss, F. J.; Sun, T. C.; Wolfart, S.; Zitzmann, N. U. Group 2 iti consensus report: Technological developments in implant prosthetics. *Clin. Oral. Implan. Res.* **2023**, *34*, 104–111.
10 Zou, W.; Li, X.; Li, N.; Guo, T.; Cai, Y.; Yang, X.; Liang, J.; Sun, Y.; Fan, Y. A comparative study of autogenous, allograft and artificial bone substitutes on bone regeneration and immunotoxicity in rat femur defect model. *Regener. Biomater.* **2021**, *8*, 1–11.
11 Chen, X.; Wu, W.; Zhu, W.; Zhou, J.; Chen, J.; Lin, Z.; Zhang, S.; Caruso, F.; Liu, C. Regulation of bone remodeling by metal–phenolic networks for the treatment of systemic osteoporosis. *ACS Appl. Mater. Interfaces* **2025**, *17*, 5995–6008.
12 Cai, M.; Yang, F.; Yang, X.; Hu, S.; Huang, L.; Hu, Y.; Jiang, X.; Liu, J. A thermoplastic and visualizable bone scaffold dynamically enhances hemostasis and osteogenesis in bone defects. *Adv. Funct. Mater.* **2026**, *36*, e31292.
13 Sadeghzade, S.; Liu, J.; Wang, H.; Li, X.; Cao, J.; Cao, H.; Tang, B.; Yuan, H. Recent advances on bioactive baghdadite ceramic for bone tissue engineering applications: 20 years of research and innovation (a review). *Mater. Today Bio* **2022**, *17*, 100473.
14 Pourhajrezaei, S.; Abbas, Z.; Khalili, M. A.; Madineh, H.; Jooya, H.; Babaeizad, A.; Gross, J. D.; Samadi, A. Bioactive polymers: A comprehensive review on bone grafting biomaterials. *Int. J. Biol. Macromol.* **2024**, *278*, 134615.
15 Zhang, J.; Jiang, Y.; Shang, Z.; Zhao, B.; Jiao, M.; Liu, W.; Cheng, M.; Zhai, B.; Guo, Y.; Liu, B.; Shi, X.; Ma, B. Biodegradable metals for bone defect repair: a systematic review and meta-analysis based on animal studies. *Bioact. Mater.* **2021**, *6*, 4027–4052.
16 Li, Y.; Wang, L.; Li, J.; Zeng, P.; Guan, S.; Yang, H.; Liu, J.; Zheng, Y. Mechanically governed fracture resistance of biodegradable zn-cu alloy stents: Role of ring-length optimized structural design. *Bioact. Mater.* **2026**, *61*, 730–742.
17 Tian, H.; Tang, Z.; Zhuang, X.; Chen, X.; Jing, X. Biodegradable synthetic polymers: Preparation, functionalization and biomedical application. *Prog. Polym. Sci.* **2012**, *37*, 237–280.
18 Tang, Z.; He, C.; Tian, H.; Ding, J.; Hsiao, B. S.; Chu, B.; Chen, X. Polymeric nanostructured materials for biomedical applications. *Prog. Polym. Sci.* **2016**, *60*, 86–128.
19 Yu, X.; Jin, X.; Huang, T.; Zhang, N.; Li, X.; Wang, Y. Poly(methyl methacrylate)-induced microstructure and hydrolysis behavior changes of poly(L-lactic acid)/carbon nanotubes composites. *Chinese J. Polym. Sci.* **2020**, *38*, 195–204.
20 Zhang, Z.; Huang, Y.; Ma, C.; Zhang, G. Progress in polymer-ceramic hybrid antifouling coatings. *Chinese J. Polym. Sci.* **2023**, *41*, 995–1001.
21 Zheng, G.; Han, L.; Ma, T.; Bian, J.; Lin, J.; Zhao, Y.; Pan, H.; Wang, Z.; Zhang, H. Synergistic effects of poly(propylene carbonate) content and pre-stretching on the strength, toughness, and heat resistance of polylactide/poly(propylene carbonate) blends. *Chinese J. Polym. Sci.* **2026**, *44*, 1142–1153.
22 Wei, J.; Sun, J.; Wang, H.; Chen, X.; Jing, X. Isothermal crystallization behavior and unique banded spherulites of hydroxyapatite/poly(l-lactide) nanocomposites. *Chinese J. Polym. Sci.* **2010**, *28*, 499–507.

Graphical Abstract

Bioinspired Zinc-doped Nano Hydroxyapatite Reinforced Poly(lactic acid) Composites for Bone Repair

Hong-Xiang Yin, Yang Wang, Yi-Fei Wu, Jin-Jing Li, Xiao Kong, Wen-Hao Mei, Ze-Tong Wang, Chun-Sheng Xiao, Cheng Zhang, Zhan-Fu Cong, Irshad Hussain, Zhao-Hui Tang, and Wei Yan

Hubei University, China; Changchun Institute of Applied Chemistry, Chinese Academy of Sciences, China; Changchun SinoBiomaterials Co., Ltd., China; Lahore University of Management Sciences (LUMS), Pakistan

Bioinspired PLA/Zn-HA composites were prepared *via* melt blending method. 10 wt% sample shows optimal mechanical performance, degradation control and bioactivity, providing promising strategy for bone repair.

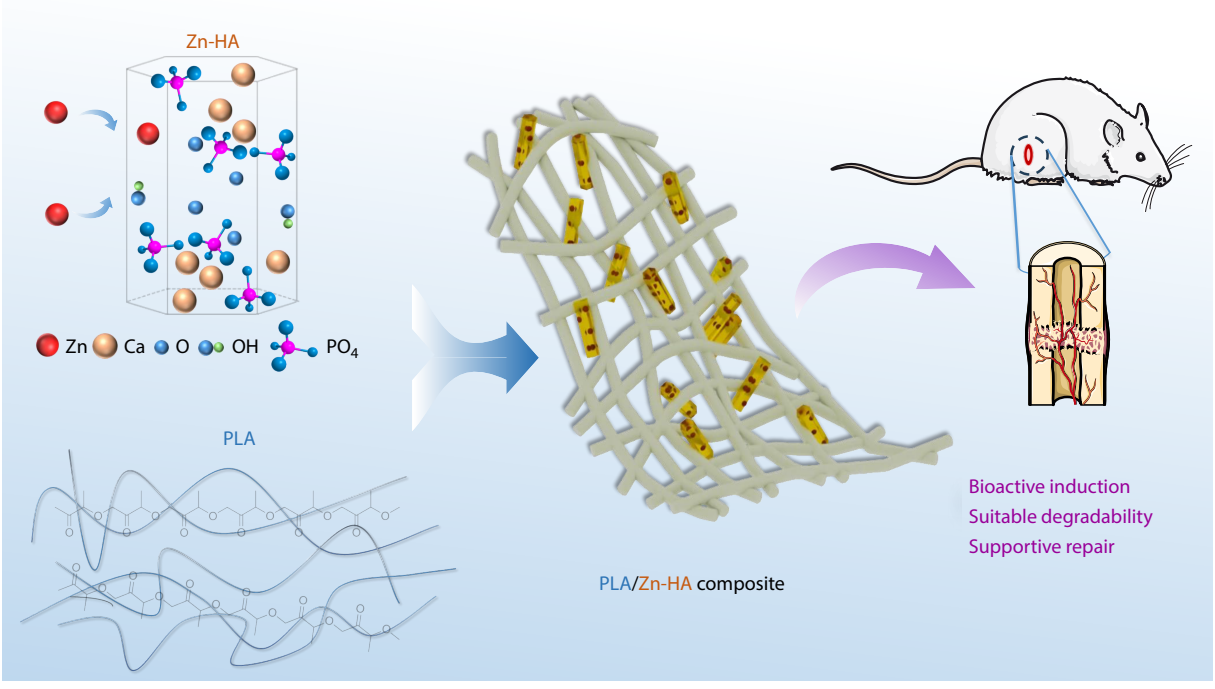

Chinese J. Polym. Sci., 2026 *https://doi.org/10.1007/s10118-026-3761-z*

23 Li, S.; Zhou, W.; Wu, W.; Shao, J.; Chen, S.; Hou, H.; Xiang, S. The crystallization behavior of L-poly(lactic acid)/polypropylene blends: the acceleration for both L-poly(lactic acid) and polypropylene. *Chinese J. Polym. Sci.* **2024**, *42*, 775–786.
24 Tian, N.; Li, Y.; Gan, H.; Ning, Z.; Jiang, N.; Gan, Z. Synergistic effect of multi-arm architecture and molecular weight on crystallization and degradation behavior of star-shaped poly(lactic acid). *Chinese J. Polym. Sci.* **2024**, *42*, 1948–1956.
25 Li, Y. P.; Shen, H.; Wang, S.; Zhang, H.; Hu, J.; Xin, R.; Sun, X.; Yan, S. Impact of annealing on the melt recrystallization of a-PDLA/α-PLLA double-layered films. *Chinese J. Polym. Sci.* **2024**, *42*, 230–238.
26 Luo, J. B.; Qiu, S.; Wang, Y.; Lai, R.; Xie, X. Preparation and physicochemical properties of hydroxyapatite/polyurethane nanocomposites. *Chinese J. Polym. Sci.* **2014**, *32*, 467–475.
27 Yan, D.; Zeng, B.; Han, Y.; Dai, H.; Liu, J.; Sun, Y.; Li, F. Preparation and laser powder bed fusion of composite microspheres consisting of poly(lactic acid) and nano-hydroxyapatite. *Addit. Manuf.* **2020**, *34*, 101305.
28 Wang, Y.; Hao, H.; Zhang, S. Lysozyme loading and release from se doped hydroxyapatite nanoparticles. *Mater. Sci. Eng.: C* **2016**, *61*, 545–552.
29 Wang, M.; You, L.; Guo, Y.; Jiang, N.; Gan, Z.; Ning, Z. Enhanced crystallization rate of poly(L-lactide)/hydroxyapatite-graft-poly(D-lactide) composite with different processing temperatures. *Chinese J. Polym. Sci.* **2020**, *38*, 599–610.
30 Zhou, P.; Wang, J.; Wang, H.; Pan, H.; Shi, H.; Fu, Y.; Yuan, Y.; Wang, Y.; Gan, Q.; Liu, C. Biomimetic 3d printing of photocrosslinkable biodegradable elastomers-modified hybrid scaffolds as instructive platforms for bone tissue regeneration. *Smart Mater. Med.* **2025**, *6*, 95–107.
31 Zhang, D.; Huang, Z.; Tong, L.; Gao, F.; Huang, H.; Chen, F.; Liu, C. Self-restoring cryogels used for the repair of hemorrhagic bone defects by modulating blood clots. *Chem. Eng. J.* **2024**, *490*, 151421.
32 Chen, S.; Wang, X.; Zhang, D.; Huang, Z.; Xie, Y.; Chen, F.; Liu, C. Tunable piezoelectric plla nanofiber membranes for enhanced mandibular repair with optimal self-powering stimulation.

Regener. Biomater. **2025**, *12*, rbae150.
33 Bai, L.; Li, J.; Li, G.; Zhou, D.; Su, J.; Liu, C. Skeletal interoception and prospective application in biomaterials for bone regeneration. *Bone Res.* **2025**, *13*, 1.
34 Pourrahmani, H.; Golparvar, M.; Fasihi, M. A new evaluation criterion for optimizing the mechanical properties of toughened polypropylene/silica nanocomposites. *Chinese J. Polym. Sci.* **2020**, *38*, 877–887.
35 Pan, H.; Wang, Y.; Jia, S.; Zhao, Y.; Bian, J.; Yang, H.; Hao, Y.; Han, L.; Zhang, H. Biodegradable poly(butylene adipate-co-terephthalate)/poly(glycolic acid) films: effect of poly(glycolic acid) crystal on mechanical and barrier properties. *Chinese J. Polym. Sci.* **2023**, *41*, 1123–1132.
36 Teng, S.; Jiang, Z.; Qiu, Z. Crystallization behavior and dynamic mechanical properties of poly(ε-caprolactone)/octaisobutyl-polyhedral oligomeric silsesquioxanes composites prepared *via* different methods. *Chinese J. Polym. Sci.* **2020**, *38*, 158–163.
37 Nishi, T.; Fujinami, S.; Wang, D.; Liu, H.; Nakajima, K. Structure and dynamics of polymeric materials in nano-scale. *Chinese J. Polym. Sci.* **2011**, *29*, 43–52.
38 Rao, W.; Li, L.; Zhang, S.; Huang, G.; Zheng, J.; Yuan, C.; Huang, Z.; Qu, J. Simultaneous improvement of strength and toughness of poly(lactic acid) *via* multiple dynamic pressure. *Chinese J. Polym. Sci.* **2025**, *43*, 1602–1615.

https://doi.org/10.1007/s10118-026-3761-z